Plasma Kallikrein Mediates Retinal Vascular Dysfunction and Induces Retinal Thickening in Diabetic Rats

Plasma Kallikrein Mediates Retinal Vascular Dysfunction and Induces Retinal Thickening in Diabetic Rats

Allen Clermont,[1,2] Tamie J. Chilcote,[3] Takeshi Kita,[1,2] Jia Liu,[1,2] Priscilla Riva,[1] Sukanto Sinha,[3] and Edward P. Feener[1,2]

OBJECTIVE—Plasma kallikrein (PK) has been identified in vitreous fluid obtained from individuals with diabetic retinopathy and has been implicated in contributing to retinal vascular dysfunction. In this report, we examined the effects of PK on retinal vascular functions and thickness in diabetic rats.

RESEARCH DESIGN AND METHODS—We investigated the effects of a selective PK inhibitor, ASP-440, and C1 inhibitor (C1-INH), the primary physiological inhibitor of PK, on retinal vascular permeability (RVP) and hemodynamics in rats with streptozotocin-induced diabetes. The effect of intravitreal PK injection on retinal thickness was examined by spectral domain optical coherence tomography.

RESULTS—Systemic continuous administration of ASP-440 for 4 weeks initiated at the time of diabetes onset inhibited RVP by 42% ($P = 0.013$) and 83% ($P < 0.001$) at doses of 0.25 and 0.6 mg/kg per day, respectively. Administration of ASP-440 initiated 2 weeks after the onset of diabetes ameliorated both RVP and retinal blood flow abnormalities in diabetic rats measured at 4 weeks' diabetes duration. Intravitreal injection of C1-INH similarly decreased impaired RVP in rats with 2 weeks' diabetes duration. Intravitreal injection of PK increased both acute RVP and sustained focal RVP (24 h postinjection) to a greater extent in diabetic rats compared with nondiabetic control rats. Intravitreal injection of PK increased retinal thickness compared with baseline to a greater extent ($P = 0.017$) in diabetic rats (from 193 ± 10 μm to 223 ± 13 μm) compared with nondiabetic rats (from 182 ± 8 μm to 193 ± 9 μm).

CONCLUSIONS—These results show that PK contributes to retinal vascular dysfunctions in diabetic rats and that the combination of diabetes and intravitreal injection of PK in rats induces retinal thickening. ***Diabetes*** **60:1590–1598, 2011**

Diabetic macular edema (DME) is a leading cause of vision loss attributed to diabetes. The 14-year incidence of this disease in individuals with type 1 diabetes followed in the Wisconsin Epidemiologic Study of Diabetic Retinopathy was 26% (1), and the progression to clinically significant macular edema was associated with increasing retinopathy severity (2). Although intensive glycemic and blood pressure control can reduce the incidence of DME (3) once this condition develops, the treatment options include laser and vascular endothelial growth factor (VEGF)-targeted therapies, which provide substantial improvement in visual acuity for ~50% of patients with DME (4). Thus, additional treatment options for this disease are needed.

DME is associated with a loss of blood-retinal barrier function, leading to increased diffusion of plasma components, thickening of the macula, and impairment in central vision (5,6). In addition to retinal thickening, increased retinal vascular permeability (RVP) alters the biochemical composition of the retinal interstitial fluid and the vitreous. Proteomic studies have begun to characterize the changes in the vitreous protein composition in people with diabetic retinopathy compared with nondiabetic subjects or diabetic subjects without diabetic retinopathy (7). We have previously reported an abundance of vasoactive plasma proteins, including components of the plasma kallikrein (PK)-kinin system (PKKS) in the vitreous of subjects with advanced diabetic retinopathy (7,8). These findings have suggested additional factors besides VEGF that may contribute to the decline in blood-retinal barrier integrity and vascular dysfunction in DME (9,10).

Plasma prekallikrein (PPK) is an abundant serine protease zymogen in blood that is converted to its catalytically active form, PK, by factor XIIa (11), contributing to the innate inflammatory response and intrinsic coagulation cascades (12). The mechanisms that lead to the activation of this pathway in vivo include interactions with polyphosphates released from activated platelets and deficiency of C1 inhibitor (C1-INH), the primary physiological inhibitor of the PKKS (13,14). PK-mediated cleavage of high-molecular weight kininogen generates the nonapeptide bradykinin (BK), which activates the BK 2 (B2) receptor. Subsequent cleavage of BK by carboxypeptidases generates des-Arg^9-BK, which activates the B1 receptor. Both B1 and B2 receptors are expressed by vascular, glial, and neuronal cell types, with the highest levels of retinal expression detected in the ganglion cell layer and inner and outer nuclear layers (15,16). Activation of B1 and B2 receptors causes vasodilation and increases vascular permeability (17–19). Previously, we have demonstrated that intravitreal injection of carbonic anhydrase-1 (CA-1) increased RVP and that this response was blocked by the inhibition of PK and by BK receptor antagonists (8). Recently, we reported that intravitreal injection of PK increased RVP in nondiabetic rats, and systemic administration of a small-molecule PK inhibitor, ASP-440, decreased RVP in rats subjected to angiotensin II (AngII)-induced hypertension (19). In the current study, we investigated the effects of PK on retinal vascular functions and retinal thickness in diabetic rats.

From the [1]Research Division, Joslin Diabetes Center, Boston, Massachusetts; the [2]Department of Medicine, Harvard Medical School, Boston, Massachusetts; and the [3]ActiveSite Pharmaceuticals, Berkeley, California.
Corresponding author: Edward P. Feener, edward.feener@joslin.harvard.edu.
Received 8 September 2010 and accepted 21 February 2011.
DOI: 10.2337/db10-1260
This article contains Supplementary Data online at http://diabetes.diabetesjournals.org/lookup/suppl/doi:10.2337/db10-1260/-/DC1.

RESEARCH DESIGN AND METHODS

Diabetes induction. Male Sprague-Dawley rats (250–300 g) were obtained from Taconic Farms (Hudson, NY). Diabetes was induced by intraperitoneal injection of streptozotocin (STZ; Sigma-Aldrich, Milwaukee, WI) in 50 mmol/L sodium citrate at 55 mg/kg after a 12-h overnight fast. Blood glucose was measured by tail sampling using a One Touch Ultra glucometer 24 h after injection of STZ. Rats with blood glucose values >250 mg/dL were considered diabetic for the study. Anesthesia used for these experiments was an intramuscular injection of ketamine (50 mg/kg; Bioniche Pharma, Lake Forest, IL) and xylazine (10 mg/kg; Sigma-Aldrich). At the conclusion of the studies, animals were killed by inhalation of carbon dioxide. The experimental protocols were approved by the Joslin Diabetes Center Institutional Animal Care and Use Committee. All animals were handled and cared for in accordance with the Association for Research in Vision and Ophthalmology Resolution on the Use of Animals in Research.

AngII-induced hypertension model. Under anesthesia, each rat was implanted with a subcutaneous Alzet osmotic pump (model 1007D, 0.5 μL/h; Durect Corporation, Cupertino, CA) containing either saline or AngII (18 μg/kg/h) and a second Alzet osmotic pump containing either saline or the PK inhibitor ASP-440 at 4 mg/mL (model 1007D, 0.5 μL/h or model 2001, 1 μL/h). Five days after pump insertion, blood pressure was measured using a noninvasive blood pressure-heart rate–monitoring system (UR-5000; Ueda Electronic, Tokyo, Japan).

Primary and secondary intervention studies with the PK inhibitor ASP-440. For the primary intervention study, diabetic and age-matched control rats were randomly assigned on day 2 after STZ injection, and diabetic rats received a subcutaneous Alzet osmotic pump (either model 2002 [0.5 μL/h] containing ASP-440 at 5 mg/mL, model 2004 [0.25 μL/h] containing ASP-440 at 24 mg/mL, or vehicle [10% polyethylene glycol/90% saline]). For the secondary intervention study, a second set of rats with STZ-induced diabetes and age-matched control rats was randomly assigned on day 14 after confirmation of diabetes and implanted with a subcutaneous Alzet osmotic pump (model 2002 [0.5 μL/h] containing ASP-440 at 12 mg/mL or vehicle [10% polyethylene glycol/90% saline]).

C1-INH intervention. After the onset of diabetes was confirmed, nondiabetic and diabetic rats that were under anesthesia received intravitreal injections of human C1-INH (200 ng/eye; EMD Chemicals, Gibbstown, NJ) in one eye and balanced salt solution (BSS) in the contralateral eye on days 2, 7, and 12. Under sterile conditions, a 31-gauge needle was inserted into the vitreous pars plana, and a 10-μL bolus of solution was slowly infused.

RVP measurements by Evans blue-dye permeation. The Evans blue-dye permeation technique was used to quantify RVP (20). In brief, under anesthesia, each animal was infused with Evans blue dye (45 mg/kg) through an indwelling jugular catheter. The dye was allowed to circulate for 2 h prior to the time the rats were killed. After tissue fixation, the eyes were enucleated. Retinas were extracted with dimethyl formamide, and the resultant supernatant was used to determine Evans blue-dye content. Results are expressed as the rate of plasma extravasation per unit weight of retinal tissue.

Retinal whole mounts. Rats with 3–4 weeks of diabetes and controls were given 10-μL intravitreal injections of human PK (hPK) (50 ng/eye; Enzyme Research, South Bend, IN) and BSS in the contralateral eye. After 24 h, 250 μL of 2×10^6 Da fluorescein isothiocyanate (FITC)-dextran (100 mg/mL FD2000S; Sigma-Aldrich) were infused into the jugular vein and allowed to circulate for 2 min. Animals were rapidly killed and the eyes enucleated. Retinas were dissected and mounted on slides with antifade mounting medium. Retinas were scanned at ×10 power, using a confocal fluorescent microscope (Zeiss Laser Scan Microscopy LSM 410).

Retinal blood flow by video fluorescein angiography. The video fluorescein angiography system, using a Rhodenstock scanning laser ophthalmoscope, has been described previously (21). In brief, the left eye of an anesthetized rat is dilated with 1% tropicamide, and a Hamilton syringe filled with 10% sodium fluorescein is attached to a jugular vein catheter. A 5-μL bolus of fluorescein is injected, and the resultant retinal angiogram is digitized and analyzed. Mean circulation time (MCT) of the dye and primary artery and vein diameter is measured at 1.5 disc diameters from the optic nerve head (ONH).

Acute RVP response to PK by vitreous fluorophotometry. To measure RVP, the eyes from rats with 4 weeks' diabetes duration and age-matched control rats were dilated and received intravitreal injections of 50 ng purified hPK in one eye and BSS in the contralateral eye. Fifteen minutes after the injection, 300 μL/kg 10% sodium fluorescein was infused via a jugular vein catheter. At 5, 15, and 25 min after dye infusion, RVP was measured by quantifying vitreous fluorescein levels by vitreous fluorophotometry (VFP), as described previously (8). We have previously shown that intravitreal injection of human serum albumin and human C1-INH does not increase RVP (8). To examine the efficacy and selectivity of the PK inhibitor, ASP-440, toward acute RVP induced by various permeability agents in nondiabetic rats, a 5-μL intravitreal injection of 20 μmol/L ASP-440 or vehicle was administered at 10 min prior to a 5-μL intravitreal injection of hPK (50 ng), VEGF (0.04 ng/μL; R&D Systems, Minneapolis, MN), or CA-1 (40 ng/μL; Sigma-Aldrich). At 10 min after the injection of the permeability agents, fluorescein dye was infused, and VFP was measured after a 30-min circulation.

Effect of exogenous PK on retinal thickness. Baseline retinal scans were made from anesthetized rats with 4 weeks' diabetes duration and age-matched controls using spectral domain–optical coherence tomography (SD-OCT) (840SDOCT System; Bioptigen, Durham, NC). Rectangular volumes of each retina were obtained consisting of 1000 A-scans by 100 B-scans over a 1.5 × 1.5 mm area centered upon the ONH. Retinal thickness was measured at 500 μm relative to the ONH at points defined by calipers on the OCT-derived en face image. At the intersection of the distance calipers and the corresponding B-scan, retinal thickness was measured using calibrated calipers from the retinal pigment epithelium (RPE) to the internal limiting membrane (ILM). Four caliper measurements were taken at each site, corresponding to the temporal, nasal, superior, and inferior quadrants of the retina. The measurements were averaged to produce a single thickness value for each retina. Retinal thickness false-color topographic maps were generated using semi-automated image segmentation software based on a smoothing filter and a Sobel operator method for edge detection in MATLAB from exported retinal OCT images. Before segmentation, a median filter was applied to reduce speckle noise and smooth the image data in the transverse direction. Edges were detected using a modified Sobel operator by taking a weighted difference. Manual input and detected boundaries in neighboring A-scans were used as constraints for the segmentation. Retinal thickness topographic maps were generated by measuring the thickness from the ILM to the posterior edge of the RPE.

PPK quantitation in plasma. Plasma was collected in citrate, and proteins were separated by SDS-PAGE. Immunoblotting was performed using an antibody against KLKB1 (LS-C38312; Lifespan Biosciences, Seattle, WA). Results were visualized by enhanced chemiluminescence (Cell Signaling, Danvers, MA). Quantification was performed using ImageQuant 5.1 (Molecular Dynamics, Sunnyvale, CA).

Statistics. Statistical analysis was performed with SigmaStat statistical software (Jandel, San Raphael, CA). Multiple group comparisons for statistical significance used Bonferroni correction for one-way ANOVA. Unpaired comparisons were made with the Student unpaired t test, and paired comparisons were made with the Student paired t test. The Mann-Whitney rank sum test was used for unequal variances. Differences were considered statistically significant when $P < 0.05$. Results are expressed as mean ± SD.

RESULTS

Effect of PK inhibition by ASP-440 on AngII-induced RVP. We examined the effective dose of ASP-440 on RVP to Evans blue dye using an AngII-induced hypertension (19). Infusion of AngII increased the systolic blood pressure (SBP) of rats compared with vehicle controls (200 ± 32 vs. 152 ± 9 mmHg, $P < 0.001$). The SBP of rats coinfused with AngII and ASP-440 at 0.2 and 0.4 mg/kg per day was 193 ± 14 and 220 ± 24 mmHg, respectively, which was not significantly different than the SBP in rats provided with AngII alone (Supplementary Table 1). AngII infusion for 7 days increased RVP by 97% compared with vehicle-treated control rats (39.6 ± 12.3 vs. 20.1 ± 3.3 μL/g/h, $P < 0.001$). Cotreatment with ASP-440 at 0.2 and 0.4 mg/kg per day decreased the AngII-mediated increase in RVP in a dose-dependent manner by 61% (27.6 ± 9.1 μL/g/h, $P = 0.015$) and 90% (22.0 ± 11.0 μL/g/h, $P = 0.002$) compared with AngII plus vehicle-treated rats (Supplementary Fig. 1). RVP was similar in vehicle- and ASP-440–treated normotensive control rats (20.1 ± 3.3 vs. 21.4 ± 8.7 μL/g/h).

Effect of PK inhibition on RVP in diabetic rats. We examined the effect of systemic administration of ASP-440 on RVP in rats with STZ-induced diabetes. Subcutaneous osmotic pumps with ASP-440 were implanted 2 days after STZ injection and delivered continuously for 4 weeks. Blood glucose and body weights were similar compared with rats receiving vehicle and ASP-440 (Supplementary Fig. 2). Diabetes increased RVP to Evans blue by 2.6-fold ($P < 0.001$) compared with age-matched control nondiabetic

rats. Treatment with ASP-440 decreased RVP in diabetic rats in a dose-dependent manner by 42% ($P = 0.013$) at 0.25 mg/kg per day and 83% ($P < 0.001$) at 0.6 mg/kg per day compared with diabetic rats that received vehicle alone (Fig. 1*A*). Next, we examined the effect of intervention with subcutaneous osmotic pumps containing ASP-440 implanted after 2 weeks' diabetes duration on RVP measured at 4 weeks' diabetes duration. RVP in diabetic rats that received ASP-440 (0.6 mg/kg per day) was decreased by 56% ($P = 0.011$) compared with diabetic rats that received vehicle (Fig. 1*B*).

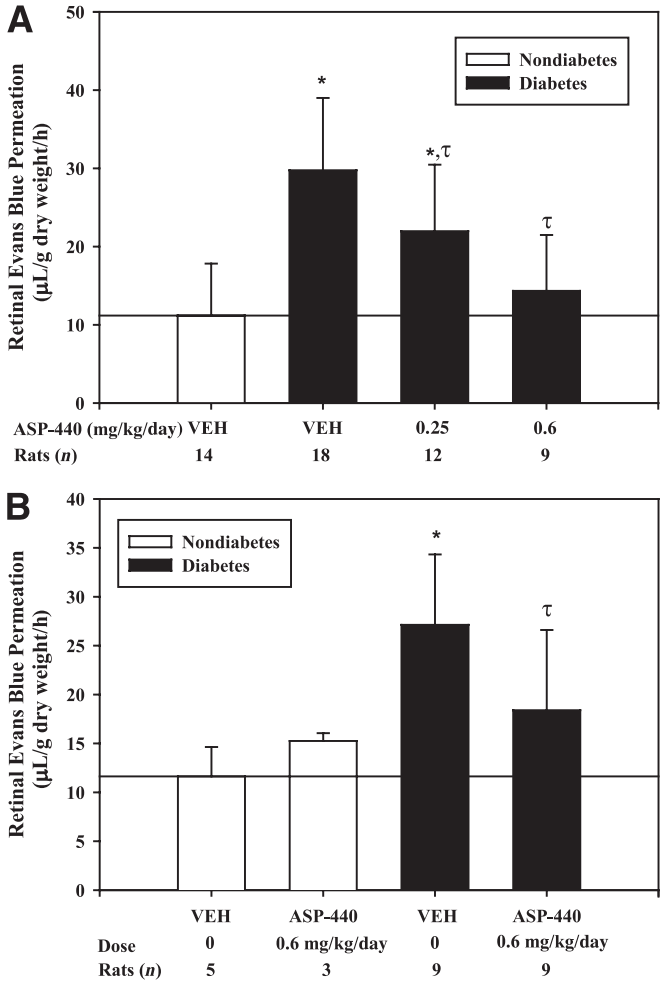

FIG. 1. ***A*: Effect of the PK inhibitor ASP-440 on RVP in rats with 4 weeks' diabetes duration and age-matched nondiabetic rats. Diabetes was induced in rats by STZ injection. After confirmation of diabetes, rats received subcutaneous osmotic pumps (Alzet model 2004) containing ASP-440 (0.25 or 0.6 mg/kg per day) or vehicle alone. Retinal Evans blue-albumin permeation was measured on day 28 after treatment. Diabetes treated with vehicle increased RVP by 2.6-fold (*$P <$ 0.001) compared with nondiabetic controls. Dosing of diabetic rats with ASP-440 at 0.25 and 0.6 mg/kg per day decreased RVP by 42% ($\tau P =$ 0.011) and 83% ($\tau P < 0.001$), respectively, compared with vehicle-treated diabetes. *B*: Effect of the PK inhibitor, ASP-440, by secondary intervention on diabetes-induced RVP in diabetic rats with 4 weeks' diabetes duration and age-matched nondiabetic rats. Two weeks after the confirmation of diabetes, rats received subcutaneous osmotic pumps (Alzet model 2002) containing ASP-440 (0.6 mg/kg per day) or vehicle alone. Retinal Evans blue-albumin permeation was measured on day 28. Diabetic rats treated with vehicle had a 2.3-fold (*$P = 0.002$) increase in RVP compared with the nondiabetic control rats. Treatment of diabetic rats with ASP-440 decreased RVP by 56% ($\tau P = 0.011$) compared with vehicle-treated diabetic rats. RVP measured in nondiabetic control rats treated with ASP-440 at 0.6 mg/kg per day was not significantly different from that measured in vehicle-treated nondiabetic control rats.**

Effects of PK inhibition on retinal hemodynamics. Retinal hemodynamics were assessed by measurements of MCT from retinal arteries to veins, measurements of primary retinal vessel diameters, and calculated RBF in rats with 4 weeks' diabetes duration in the absence or presence of treatment from week 2 to 4 with ASP-440. We show that MCT was prolonged ($P < 0.001$) and RBF was decreased ($P = 0.001$) in diabetic rats compared with nondiabetic control rats (Fig. 2), as described previously (22). Intervention with ASP-440 resulted in partial normalization of the diabetes-induced retinal hemodynamic changes, decreasing MCT ($P = 0.015$) and increasing RBF ($P = 0.001$) compared with diabetic rats that received vehicle alone. ASP-440 treatment in diabetic rats was also associated with increased diameter of retinal arteries (9.7 ± 0.7 vs. 8.7 ± 0.7 pixels, $P = 0.011$) and veins (13.3 ± 0.8 vs. 12.3 ± 0.7 pixels, $P = 0.03$) compared with diabetic rats that received vehicle alone.

Circulating PPK levels in diabetes. PPK levels in plasma from both diabetic and nondiabetic rats were quantified. We show that PPK protein levels measured by immunoblot were increased by 74% ($P = 0.005$) in diabetic rats and 64% ($P = 0.027$) in ASP-440–treated diabetic rats compared with nondiabetic rats (Supplementary Fig. 3).

Effect of C1-INH on RVP in diabetic rats. C1-INH is the primary physiological inhibitor of PK and plays a critical role in suppressing plasma extravasation in areas of local inflammation (14,23). We examined the effect of intravitreal injection of C1-INH on RVP in both diabetic and nondiabetic rats. RVP assessed by Evans blue-dye permeation was increased after 2 weeks of diabetes compared with nondiabetic controls (Fig. 3). We show that eyes that received an intravitreal injection of C1-INH (200 ng) at

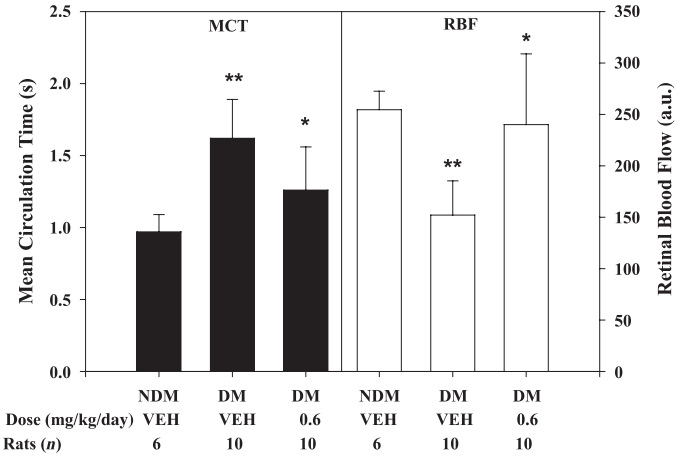

FIG. 2. Effect of ASP-440 by secondary intervention on diabetes-mediated retinal hemodynamics. Diabetes was induced in rats by STZ injection. Two weeks after the confirmation of diabetes, rats received subcutaneous osmotic pumps (Alzet model 2002) containing ASP-440 (0.6 mg/kg per day) or vehicle alone. After 4 weeks' diabetes duration, retinal hemodynamics was measured by VFA. MCT of fluorescein dye transit was measured from retinal angiograms. Primary vessel diameters were measured by boundary-crossing algorithm. RBF was calculated from the average of segmental blood flows. Diabetes (DM) increased MCT by 1.5-fold ($P < 0.001$) and decreased RBF by 40% (**$P = 0.001$) compared with nondiabetic (NDM) controls. Treatment of diabetes with ASP-440 improved MCT by 55% (*$P = 0.015$) and RBF by 86% (*$P = 0.001$), respectively, compared with vehicle (VEH)-treated diabetes alone. a.u., arbitrary unit.**

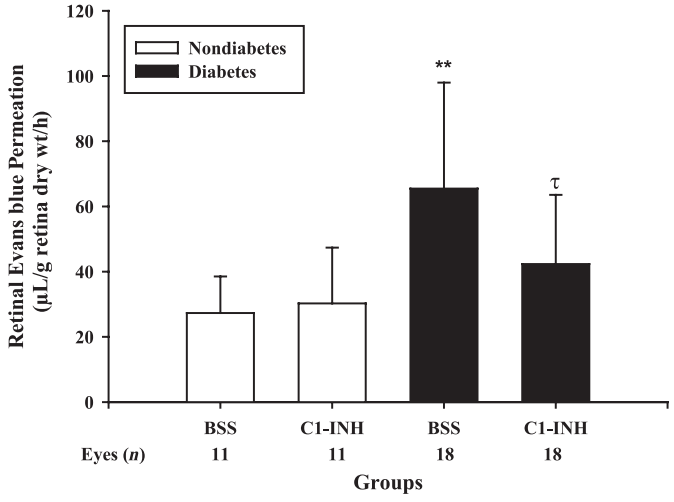

FIG. 3. Effect of C1-INH interventional treatment on diabetes-induced RVP. Diabetes was induced in rats by STZ injection. After confirmation of diabetes, rats were given 10-μL intravitreal injections of C1-INH (200 ng/eye) and BSS in the contralateral eye on days 2, 7, and 12. Retinal Evans blue-albumin permeation was measured on day 14 after diabetes onset. Diabetes treated with BSS increased RVP by 2.4-fold (P < 0.001) compared with nondiabetic controls. Treatment of diabetes with C1-INH decreased RVP by 61% (τP = 0.003) compared with BSS-treated diabetes. Treatment of nondiabetic controls with C1-INH had no effect compared with nondiabetic BSS controls.**

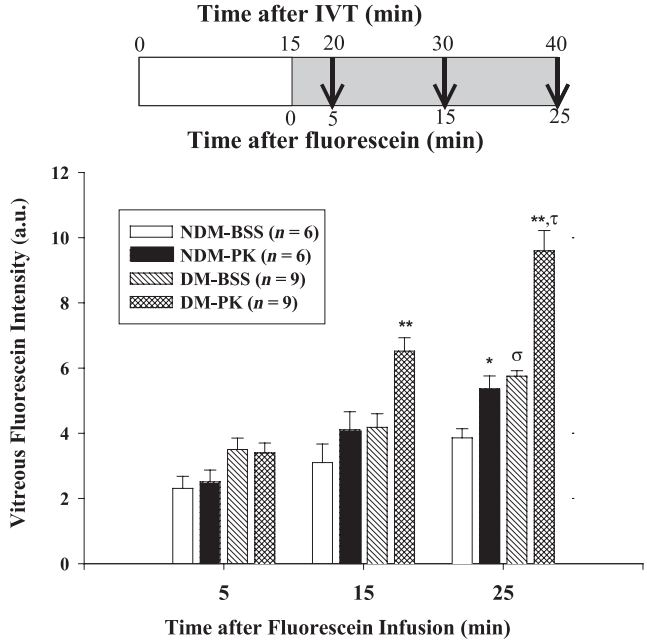

FIG. 4. Effect of exogenous PK on RVP in 4 weeks' diabetes (DM) duration and age-matched nondiabetic (NDM) rats. Diabetes was induced in rats by STZ injection. After 4 weeks of diabetes, rats were given 10-μL intravitreal (IVT) injections of hPK (50 ng/eye) and BSS in the contralateral eye. After 15 min, a bolus of 10% sodium fluorescein was infused into the jugular vein. Leakage of fluorescein was measured in the vitreal compartment by VFP at 5, 15, and 25 min after bolus infusion. At 5 min after infusion, no difference was observed between PK and BSS eyes for diabetes or nondiabetes. At 15 min postinfusion, PK-induced leakage was 33 and 56% (P < 0.001) greater than the BSS-injected eye in nondiabetic and diabetic rats, respectively. At 25 min postinfusion, diabetes with BSS leakage was greater than nondiabetes-injected BSS (σP < 0.001). PK-induced leakage was 34% (*P < 0.01) and 67% (**P < 0.001) greater than the BSS-injected eye in nondiabetic and diabetic rats, respectively. The increase in PK-induced leakage compared with BSS injection was greater in diabetic rats (τP = 0.037) than in nondiabetic rats, indicating an increased retinal sensitivity to the presence of PK. a.u., arbitrary unit.**

days 2, 7, and 12 after diabetes onset displayed a 61% (P = 0.003) decrease in RVP compared with contralateral eyes that received control injections with saline vehicle. Intravitreal injection of C1-INH did not significantly affect RVP in nondiabetic rats.

Effects of intravitreal injection of PK on RVP. We examined the effects of intravitreal injection of PK, compared with vehicle, on RVP in diabetic and nondiabetic rats. We estimated the vitreous volume to be ~100 μL and injected 50 ng hPK per eye. This concentration of PK in the vitreous is comparable with 0.5 ng/μL PK levels that we have detected in human diabetic retinopathy vitreous (data not shown). We demonstrate that intravitreal injection of hPK increased RVP in both nondiabetic and diabetic rats, compared with eyes that received saline vehicle injections (Fig. 4). It is noteworthy that we found that the magnitude of RVP increase induced by intravitreal injection of hPK in diabetic rats was significantly greater than that observed in nondiabetic rats (67 ± 30 vs. 34 ± 19%, P = 0.037).

We next examined the effect of intravitreal injections of ASP-440 or vehicle on RVP in nondiabetic rats induced by subsequent intravitreal injections with hPK, CA-1, and VEGF. Intravitreal injection with ASP-440 (20 μmol/L) pretreatment decreased PK- and CA-1-induced RVP by 75 and 73% (P < 0.001), respectively, compared with PK and CA-1 alone (Fig. 5). In contrast, ASP-440 did not alter VEGF-induced RVP. These findings confirm that PK inhibition blocks CA-1-mediated RVP (8) but not VEGF-mediated RVP, which has been shown to be inhibited by >95% after intravitreal injection of the protein kinase Cβ inhibitor, LY333531 (24). These results suggest that ASP-440's inhibition of either AngII-induced RVP or diabetes-induced RVP proceeds via inhibition of endogenous PK and not via a direct effect on endogenous VEGF or protein kinase Cβ.

The effects of PK on RVP were also assessed 24–48 h postinjection by visualizing the leakage of FITC-dextran (molecular mass 2×10^6 Da) conjugate. We show that eyes subjected to intravitreal injection of PK displayed focal areas of leakage to FITC-dextran that were not observed in retinas from eyes that received saline vehicle injection (Fig. 6). At least one area of focal leakage was observed on retinal whole mounts in five of eight eyes injected with PK compared with none of eight saline vehicle–injected eyes in diabetic rats, indicating a sustained effect of intravitreal PK on focal leakage. In nondiabetic rats, eyes injected with PK had at least one area of focal leakage in two of eight eyes compared with none of eight eyes injected with saline vehicle. These findings show that intravitreal injection of PK induced sustained focal leakage in both nondiabetic and diabetic rats, with a trend for more leakage in diabetic rats.

Effect of intravitreal injection of PK on retinal thickness. The effects of diabetes and intravitreal PK injection on retinal thickness were examined using SD-OCT. OCT scans were obtained for each retina at baseline and at 24 h postinjection. Retinal thickness measurements were registered using en face images relative to the center of the ONH (Figs. 7*A*–*D*). Representative en face images and a corresponding B-scan at 500 μm superior to the ONH are shown in Fig. 7 at 24 h postinjection for nondiabetic and diabetic rats that received BSS (Fig. 7*A* and *C*) or PK (Fig. 7*B* and *D*). B-scans illustrate a single caliper measurement from RPE to ILM at the 500-μm intersection point.

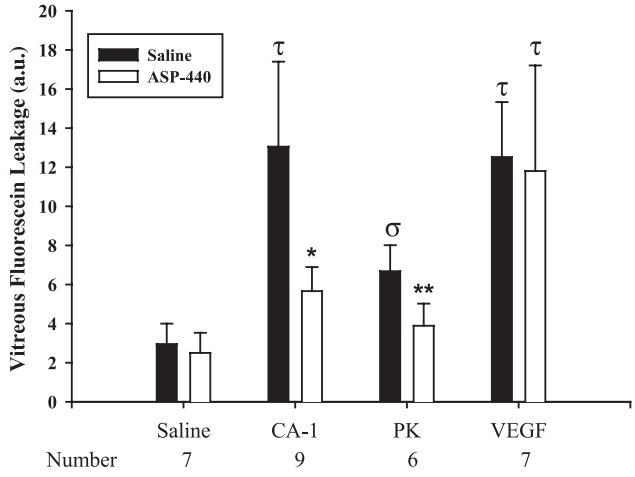

FIG. 5. Effect of ASP-440 on PK-, CA-1-, and VEGF-induced RVP. Nondiabetic rats were given 5-μL intravitreal injections of ASP-440 (20 μmol/L) and vehicle in the contralateral eye. After 10 min, a second 5-μL intravitreal injection of either CA-1 (200 ng/eye), PK (50 ng/eye), or VEGF (0.2 ng/eye) was given in both eyes. After an additional 10 min, a bolus of fluorescein dye was infused into the jugular vein. At 30 min after dye infusion, leakage of fluorescein was measured in the vitreal compartment by VFP. CA-1 and VEGF increased RVP by 3.1- and 4-fold, respectively, compared with vehicle control (τP < 0.001). Pretreatment with ASP-440 decreased CA-1–induced RVP by 75% (*P < 0.001) but had no effect on VEGF-induced RVP. PK increased RVP by 126% compared with vehicle control (σP < 0.05), and pretreatment with ASP-440 blocked this effect by 73% (P < 0.001). a.u., arbitrary unit.**

Observations from the en face images indicated that PK injection induced vascular dilation and tortuosity that were not evident in the BSS control retina. Baseline retinal thickness in nondiabetic and diabetic rats were 182 ± 8 and 193 ± 10 μm, respectively (P = 0.024) (Fig. 7*E*). The reproducibility of measurements from consecutively acquired SD-OCT images was 1.2 ± 1.0 μm. Retinal thickness in nondiabetic rats 24 h postintravitreal injection of BSS or PK was 189 ± 4 and 193 ± 9 μm, respectively. Retinal thicknesses in diabetic rats following BSS or PK intravitreal injection was higher at 196 ± 8 and 223 ± 13 μm (P < 0.01), respectively. Results are summarized in Supplementary Table 2.

To further evaluate the regions of retinal thickness, an edge-detection algorithm was applied to each B-scan to identify the RPE and ILM boundaries. Point differences between layers were measured along each B-scan, and the results were compiled to create a retinal-thickness map. Representative thickness maps for corresponding baseline and 24-h post-PK injection are shown for nondiabetes (Fig. 8*A* and *B*) and diabetes (Fig. 8*C* and *D*), respectively. Automated segmentation was not possible near the ONH because of the absence of the RPE as a reference position and the presence of hyaloid remnants. This region is indicated in white. Thickness false-color topographic maps illustrate diffuse PK-induced thickening throughout the retina in both nondiabetic and diabetic rats. These thickness topographic maps also show increased retinal thickness coincident with primary vessels, which appeared elevated above the plane of the nerve fiber layer and approximately uniform thickness between these vessels on the 500-μm annulus in the inferior-superior and nasal-temporal axes, corresponding to the locations of caliper measurements indicated in Fig. 7.

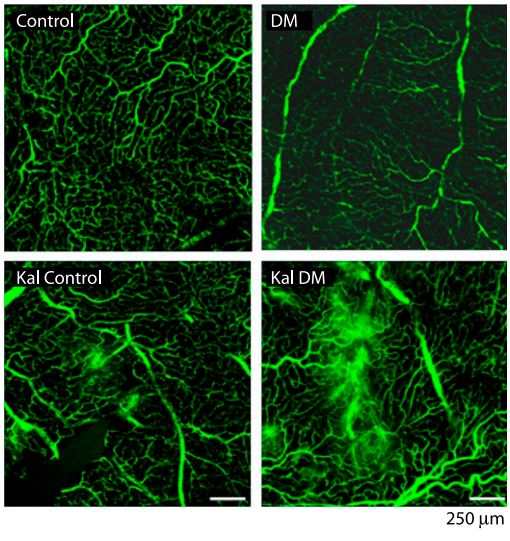

FIG. 6. Exogenous intravitreal PK (Kal) induces focal retinal leakage of FITC-labeled dextran at 24 h after injection. After 4 weeks' diabetes duration, both diabetic (DM) and age-matched nondiabetic control rats were given 10-μL intravitreal injections of PK (50 ng/eye) and BSS in the contralateral eye. After 24 h, 250 μL 2 × 10^6 Da FITC-dextran (100 mg/mL) was infused into the jugular vein and allowed to circulate for 2 min. Retinal whole mounts were prepared and imaged by confocal microscopy. Nondiabetic control and diabetic eyes injected with BSS display an intact vascular bed at 24 h postinjection. PK-injected eyes display small focal areas of dextran extravasation in nondiabetic control and larger focal areas in diabetic retina. (A high-quality digital representation of this figure is available in the online issue.)

DISCUSSION

This report provides the first characterization of the effect of PK inhibition on retinal vascular dysfunction in diabetes and the effect of intravitreal injection of PK on retinal thickness. We show that systemic administration of a selective small-molecule PK inhibitor, ASP-440 (19), ameliorated both RVP and RBF abnormalities in diabetic rats. Using a prevention protocol, continuous delivery of ASP-440 for 4 weeks inhibited diabetes-induced increased RVP by >80% without altering blood glucose or body weight. Using an intervention protocol, we show that ASP-440 inhibited diabetes-induced RVP when treatment was initiated 2 weeks after diabetes onset, although this did not affect RVP compared with baseline in nondiabetic normal rats. The efficacious dose range of ASP-440 in diabetic rats was comparable with that observed in rats with 7 days of AngII-induced hypertension. Although ASP-440 inhibited PK-induced RVP, it did not affect VEGF-induced RVP, suggesting that its beneficial effects on pathological RVP are not a result of a direct inhibition of VEGF-induced blood-retinal barrier permeability. These findings suggest that PK activity contributes to the elevated levels of RVP associated with both hyperglycemia and hypertension, both of which are major risk factors for diabetic retinopathy progression and DME (1,3), and also that systemic PK inhibition does not alter RVP in normal, healthy animals. We also show that intravitreal injection of C1-INH decreased RVP in diabetic rats, suggesting that local intraocular activation of the PKKS contributes to increased RVP in diabetic rats. We have previously shown that intravitreal injection of C1-INH blocked CA-1–induced RVP (8), suggesting that PK inhibition may also reduce RVP associated with retinal hemorrhages, which often increase in number and severity during diabetic retinopathy progression.

The effects of the PKKS on vascular permeability at sites of vascular injury and inflammation have been attributed

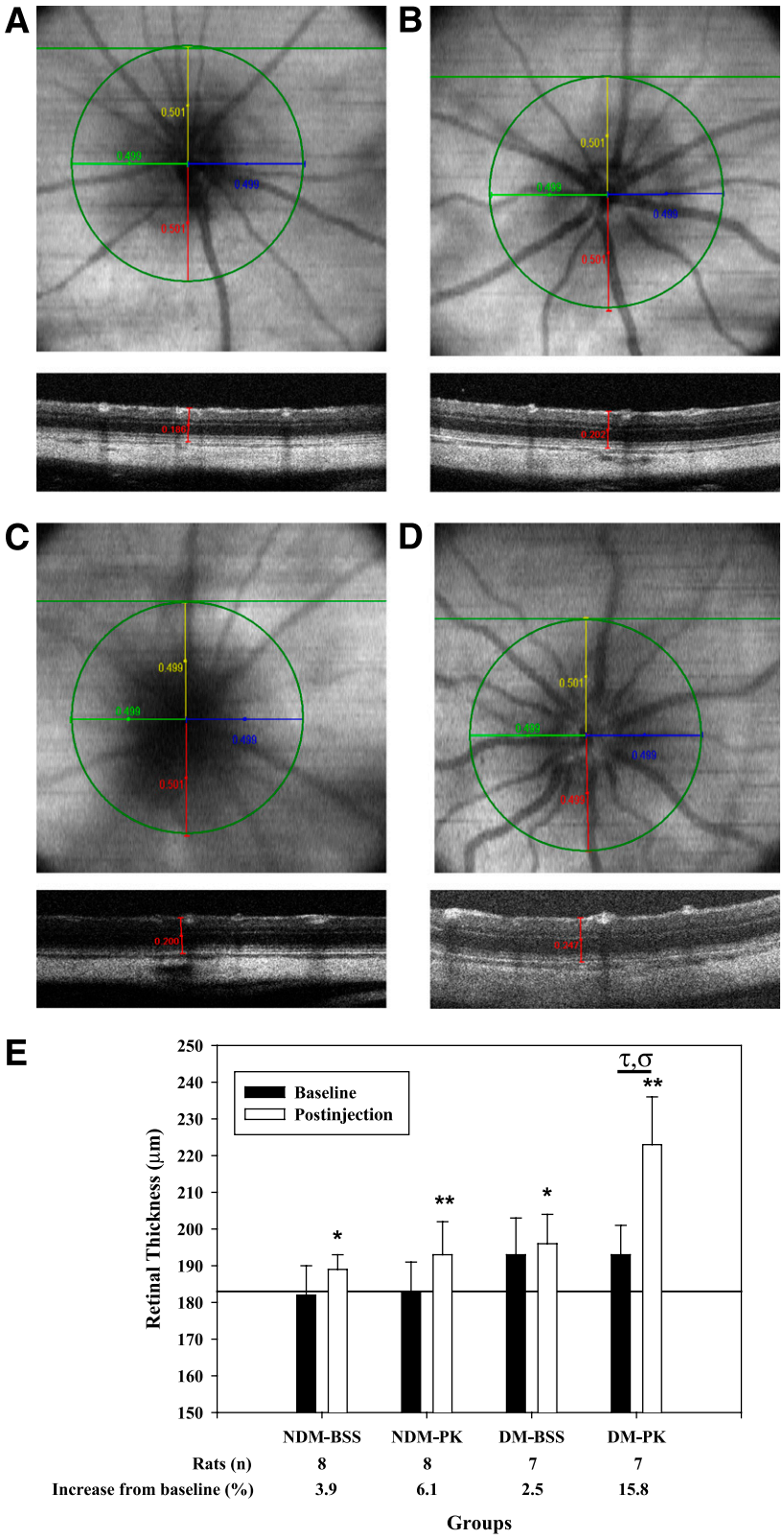

FIG. 7. Representative en face OCT and B-scan images of rat retina obtained by spectral domain optical coherence tomography (SD-OCT) at 24 h after intravitreal injection and resultant retinal thickness measurements. After 4 weeks' diabetes duration, baseline SD-OCT scans of the retina from each eye were obtained (100 B-scans of 1,000 A-scans over a 1.5 × 1.5 mm area). Rats were given 10-μL intravitreal injections of PK (50 ng/eye) and BSS in the contralateral eye. At 24 h after injection, repeat SD-OCT scans of the retina from each eye were obtained. *A–D*: The center of the optic nerve was identified, and a 500-μm radius was drawn on the en face image as shown in. The intersection of the radii terminus and the corresponding B-scan identified the retinal sites for thickness measurement. Retinal thickness was measured on the intersecting B-scan from the RPE to the ILM using calipers calibrated in microns. En face images were saved for retinal registration between timed SD-OCT scans. En face and B-scan slices are shown for nondiabetes (NDM) plus BSS (*A*), nondiabetes plus PK (*B*), diabetes (DM) plus BSS (*C*), and diabetes plus PK (*D*). B-scans correspond to the horizontal green line shown on each en face image. A single caliper is drawn on the corresponding B-scan at the 500-μm point from the ONH. B-scans of PK-treated nondiabetic and diabetic retina illustrate increased thickness compared with BSS alone. En face images

to the production and actions of BK peptides (12,14). Both B1 and B2 receptors are expressed in retina, and their direct activation via intravitreal injections of BK and des-Arg^9-BK, respectively, has been shown to increase RVP (17,19). Abdouh et al. (17) have shown that retinal B1 receptor expression and des-Arg^9-BK–induced RVP were increased in diabetic rats compared with nondiabetic controls and that 7 days of systemic treatment with a B1 receptor antagonist significantly reduced diabetes-induced RVP. Likewise, Lawson et al. (25) reported that B1 receptor antagonism decreased RVP in Wistar rats with 4 weeks of STZ-induced diabetes. These reports suggest that activation of the PKKS can increase RVP via both B1 and B2 receptors and that diabetes appears to increase actions mediated via the B1 receptor. However, although upregulation of retinal B1 receptors has been demonstrated in rodent models with short duration of diabetes (17,26), there is no information currently available on retinal B1 receptor expression levels in diabetic retinopathy in humans. Kedzierska et al. (27) have reported that circulating PPK levels are elevated in people with diabetic retinopathy. In the current study, we show that PPK levels in the plasma of diabetic rats were elevated compared with nondiabetic control rats (Supplementary Fig. 3), which is consistent with previous findings using STZ-induced diabetic Wistar rats (28,29). Lawson et al. (25,30) have shown that systemic administration of the B1 antagonist R-954 in diabetic rats decreased vascular permeability in other organs, including aorta, heart, kidney, and skin. Taken together, these findings suggest that systemic activation of the PKKS may contribute to increased vascular permeability in multiple tissues that are associated with diabetic vasculopathies.

We have previously shown that the retinal MCT, which measures the rate of hemodynamics across the retinal microvasculature, is prolonged, and the RBF is decreased in diabetic rats with 2 weeks of STZ-induced diabetes (22). In this report, we show that the abnormalities in MCT and RBF were significantly ameliorated in rats that received ASP-440 for 2 weeks in the interventional protocol. It is surprising that we found that ASP-440 increased retinal vessel diameters in diabetic rats, suggesting that activation of endogenous PK in diabetic rats leads to vasoconstriction of retinal vessels. Although acute administration of BK has been shown to increase retinal vessel diameters (26), the effects of chronic PK activation and increased RVP on retinal hemodynamics are not yet known. Although the role of retinal hemodyamics on the pathology of diabetic retinopathy is not fully understood, decreases in RBF have been described for diabetic patients with no diabetic retinopathy or mild nonproliferative diabetic retinopathy (31–33), suggesting that it is associated with early retinal vascular responses to diabetes and diabetic retinopathy. The reduction in RVP and the increase in RBF observed in diabetic rats that received ASP-440 compared with vehicle-treated diabetic controls show that PK inhibition ameliorates two early retinal vascular abnormalities caused by diabetes.

We have reported previously (7,8) that PK, high-molecular weight kininogen, and FXII are present at elevated levels in vitreous fluid obtained from people with diabetic retinopathy. The vitreous in diabetic retinopathy contains a number of proteins that have been shown to bind and activate components of the PKKS, including collagen and laminin (34,35), misfolded proteins (36), CA-1 (8), and heat shock protein 90 (7,37). We have shown a high ratio of PK relative to PPK in diabetic retinopathy vitreous (8), suggesting that PPK within the vitreous is efficiently activated to PK. Although the mechanisms contributing to PKKS expression in the vitreous are not fully understood, increased RVP in diabetes could enable diffusion of PKKS components from the blood to the retinal interstitial fluid and into the vitreous. In this report, we demonstrate that the magnitude of the acute increase in RVP to fluorescein and the prolonged increase in focal areas of RVP to FITC-dextran conjugate 24 h post-PK intravitreal injection were greater in diabetic rats compared with nondiabetic controls. Recently, using a proteomics approach, we have shown that PK induces the proteolysis of extracellular matrix proteins released from astrocytes, including collagen, fibronectin, laminin, and nidogen (38). These findings suggest that PK-induced proteolysis of basement membrane may contribute to its sustained effects on the retina.

We demonstrate that intravitreal injection of PK in diabetic rats results in an increase in retinal thickness measured using SD-OCT. We used two methods to evaluate retinal thickness using SD-OCT data collected at baseline and at 24 h after intravitreal injection. The first method involved the generation of a 500-μm annulus on the fundus image centered on the ONH that was used to define four regions for retinal thickness measurements from B slices using calipers. By use of this approach, we were able to perform image registration for pre- and post-injection measurements of retinal thickness. This method enabled reproducibility of retinal-thickness measurements with a tolerance of 1–2 μm. In the second method, we used an algorithm to automate segmentation of B slices and compiled thickness data to generate thickness topographic maps. Thicknesses were visualized using a colored-scale heat map centered at 200 μm. This method provided the advantage of a wider field of visualization of retinal thickness compared with the caliper approach described above. These thickness maps indicated that PK-induced retinal thickening was relatively uniform in all quadrants of the retina. We show that PK intravitreal injection in diabetic rats resulted in a marked increase in thickness compared with both baseline measurements and to the response observed in nondiabetic rats, a response consistent with the PK-induced changes in RVP. Our results suggest that the level of RVP induced by diabetes alone may not be sufficient to induce a robust increase in retinal thickness in rats. This is consistent with clinical findings that have demonstrated a correlation between DME and the severity of RVP (39). Previous studies based on vitreous proteomics have suggested that RVP and hemorrhage can

show vessel tortuosity and vascular dilation of the primary vasculature after PK injection compared with BSS-treated retina. *E*: Quantification of retinal thickness in diabetic and age-matched nondiabetic rats at baseline and 24 h after intravitreal injection of PK. Diabetes was induced in rats by STZ injection. After 4 weeks of diabetes, baseline SD-OCT scans of the retina from each eye were obtained. Rats were given 10-μL intravitreal injections of PK (50 ng/eye) and BSS in the contralateral eye. At 24 h postinjection, follow-up SD-OCT scans of the retina from each eye were obtained. For BSS-treated eyes, retinal thickness increased at 24 h by 3.9% (*$P < 0.05$) and 2.5% (*$P < 0.05$) compared with baseline thickness in nondiabetic and diabetic rats, respectively. For PK-treated eyes, retinal thickness increased at 24 h by 6.1% ($P < 0.01$) and 15.8% ($P < 0.01$) compared with baseline thickness in nondiabetic and diabetic rats, respectively. The increase in retinal thickness by PK in diabetes was greater than the change observed in the contralateral BSS injection alone ($\tau P = 0.002$) and was greater than the effect of PK on thickness in nondiabetes ($\sigma P = 0.017$). (A high-quality digital representation of this figure is available in the online issue.)**

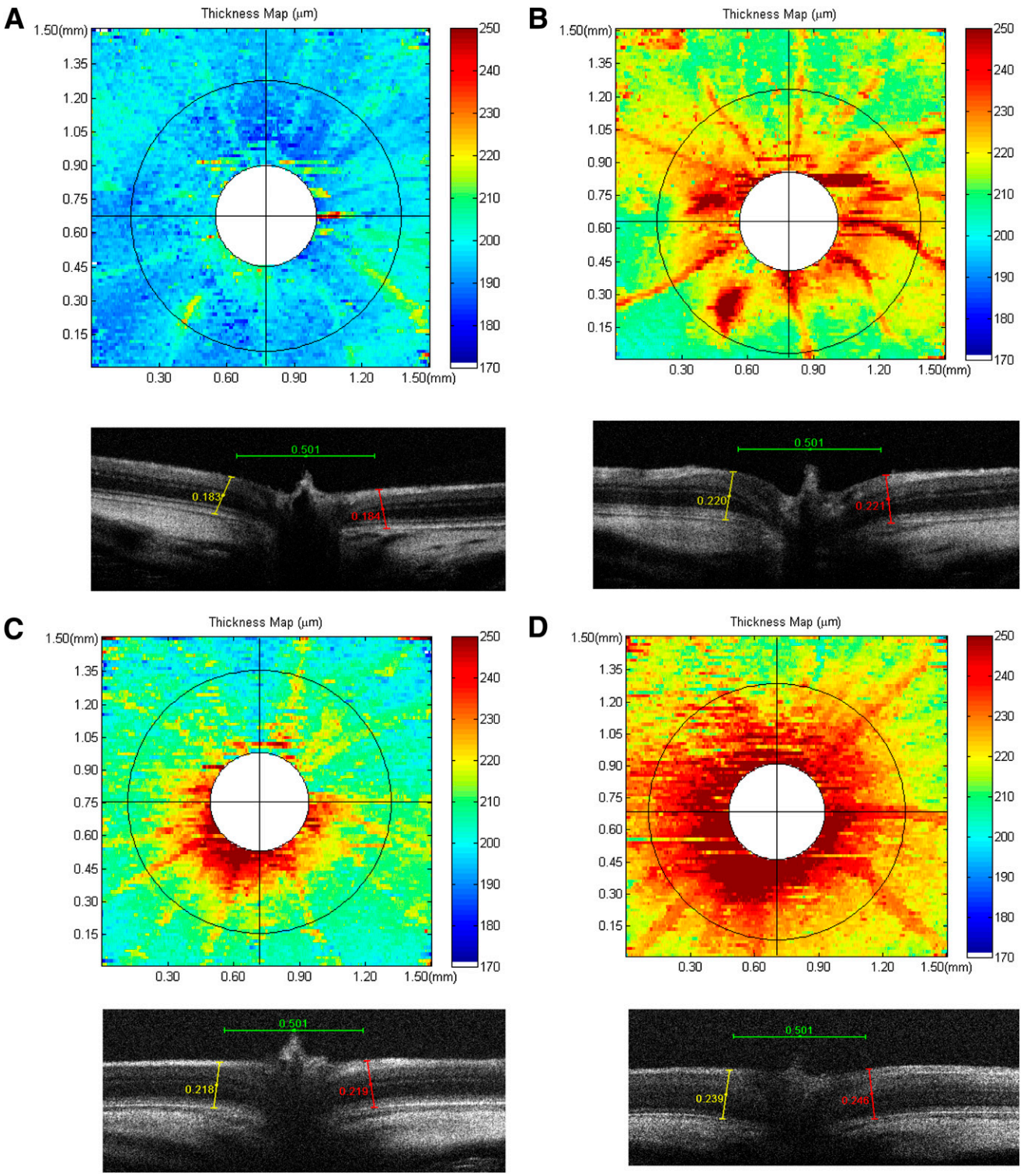

FIG. 8. Representative false-color topographic thickness maps of rat retina obtained by SD-OCT illustrating the effect of exogenous PK on the retina at 24 h after injection into the vitreous. Thickness maps were generated by using an edge-detection algorithm to identify the RPE and ILM layers in each horizontal B-scan of a rectangular retinal volume. Thickness was calculated as a difference between points on the RPE and ILM along an entire B-scan. Baseline and 24 h after PK injection thickness maps are shown for nondiabetic (*A* and *B*) and diabetic (*C* and *D*) rats, respectively. Corresponding B-scans bisecting the ONH from each map are shown below. Exogenous PK increased retinal thickness uniformly across the retina in both nondiabetes and diabetes and induced vascular dilation, as indicated by increased vessel thickness. B-scans illustrate an increase in retinal thickness at the ONH rim at baseline and enhanced thickness at the ONH induced by PK at 24 h after injection. (A high-quality digital representation of this figure is available in the online issue.)

activate pathways that are additive to those induced by diabetes alone and that this additive effect may overwhelm compensatory mechanisms that mediate retinal fluid balance (8). Our results suggest that increased PK levels in the vitreous may be one of the factors that contribute to retinal thickening in diabetes.

In conclusion, this report shows that inhibition of PK reduces RVP in diabetic rats and describes a new model of

retinal thickening that is generated by the intravitreal injection of PK in diabetic rats. These findings suggest that either systemic administration of a small-molecule PK inhibitor, such as ASP-440, or intravitreal injection of C1-INH, a physiological PK inhibitor, may provide new pharmaceutical treatment options to reduce RVP associated with diabetic retinopathy and DME.

ACKNOWLEDGMENTS

This work was supported in part by the Juvenile Diabetes Foundation International and the National Institutes of Health (grants EY-19029, DK-36836, and HL-090132).

T.J.C. and S.S. are cofounders of ActiveSite Pharmaceuticals. The Joslin Diabetes Center and ActiveSite Pharmaceuticals have filed a patent application on the methods for treatment of kallikrein-related disorders. No other potential conflicts of interest relevant to this article were reported.

A.C. researched data and prepared the manuscript. T.J.C. and S.S. provided reagents, edited the manuscript, and contributed to the discussion. T.K. edited the manuscript. T.K., J.L., and P.R. researched data. E.P.F directed and supervised the entire study and contributed to manuscript writing.

The authors thank Matthew Bokhari, Joslin Diabetes Center, for excellent technical assistance; Dr. James Fujimoto and Jonathan Liu, Research Laboratory of Electronics at the Massachusetts Institute of Technology, Cambridge, MA, for their expertise with SD-OCT; and Chris Cahill, Joslin Diabetes Center, of the Microscopy Core.

REFERENCES

1. Klein R, Klein BE, Moss SE, Cruickshanks KJ. The Wisconsin Epidemiologic Study of Diabetic Retinopathy: XVII: the 14-year incidence and progression of diabetic retinopathy and associated risk factors in type 1 diabetes. Ophthalmology 1998;105:1801–1815
2. Henricsson M, Sellman A, Tyrberg M, Groop L. Progression to proliferative retinopathy and macular oedema requiring treatment: assessment of the alternative classification of the Wisconsin Study. Acta Ophthalmol Scand 1999;77:218–223
3. Mohamed Q, Gillies MC, Wong TY. Management of diabetic retinopathy: a systematic review. JAMA 2007;298:902–916
4. Elman MJ, Aiello LP, Beck RW, et al.; Diabetic Retinopathy Clinical Research Network. Randomized trial evaluating ranibizumab plus prompt or deferred laser or triamcinolone plus prompt laser for diabetic macular edema. Ophthalmology 2010;117:1064–1077.e35
5. Kang SW, Park CY, Ham DI. The correlation between fluorescein angiographic and optical coherence tomographic features in clinically significant diabetic macular edema. Am J Ophthalmol 2004;137:313–322
6. Antonetti DA, Barber AJ, Bronson SK, et al.; JDRF Diabetic Retinopathy Center Group. Diabetic retinopathy: seeing beyond glucose-induced microvascular disease. Diabetes 2006;55:2401–2411
7. Gao BB, Chen X, Timothy N, Aiello LP, Feener EP. Characterization of the vitreous proteome in diabetes without diabetic retinopathy and diabetes with proliferative diabetic retinopathy. J Proteome Res 2008;7:2516–2525
8. Gao BB, Clermont A, Rook S, et al. Extracellular carbonic anhydrase mediates hemorrhagic retinal and cerebral vascular permeability through prekallikrein activation. Nat Med 2007;13:181–188
9. Phipps JA, Feener EP. The kallikrein-kinin system in diabetic retinopathy: lessons for the kidney. Kidney Int 2008;73:1114–1119
10. Feener EP. Plasma kallikrein and diabetic macular edema. Curr Diab Rep 2010;10:270–275
11. Iwaki T, Castellino FJ. Plasma levels of bradykinin are suppressed in factor XII-deficient mice. Thromb Haemost 2006;95:1003–1010
12. Joseph K, Kaplan AP. Formation of bradykinin: a major contributor to the innate inflammatory response. Adv Immunol 2005;86:159–208
13. Müller F, Mutch NJ, Schenk WA, et al. Platelet polyphosphates are proinflammatory and procoagulant mediators in vivo. Cell 2009;139:1143–1156
14. Han ED, MacFarlane RC, Mulligan AN, Scafidi J, Davis AE 3rd. Increased vascular permeability in C1 inhibitor-deficient mice mediated by the bradykinin type 2 receptor. J Clin Invest 2002;109:1057–1063
15. Ma JX, Song Q, Hatcher HC, Crouch RK, Chao L, Chao J. Expression and cellular localization of the kallikrein-kinin system in human ocular tissues. Exp Eye Res 1996;63:19–26
16. Yasuyoshi H, Kashii S, Zhang S, et al. Protective effect of bradykinin against glutamate neurotoxicity in cultured rat retinal neurons. Invest Ophthalmol Vis Sci 2000;41:2273–2278
17. Abdouh M, Talbot S, Couture R, Hasséssian HM. Retinal plasma extravasation in streptozotocin-diabetic rats mediated by kinin B(1) and B(2) receptors. Br J Pharmacol 2008;154:136–143
18. Jeppesen P, Aalkjaer C, Bek T. Bradykinin relaxation in small porcine retinal arterioles. Invest Ophthalmol Vis Sci 2002;43:1891–1896
19. Phipps JA, Clermont AC, Sinha S, Chilcote TJ, Bursell SE, Feener EP. Plasma kallikrein mediates angiotensin II type 1 receptor-stimulated retinal vascular permeability. Hypertension 2009;53:175–181
20. Xu Q, Qaum T, Adamis AP. Sensitive blood-retinal barrier breakdown quantitation using Evans blue. Invest Ophthalmol Vis Sci 2001;42:789–794
21. Bursell SE, Takagi C, Clermont AC, et al. Specific retinal diacylglycerol and protein kinase C beta isoform modulation mimics abnormal retinal hemodynamics in diabetic rats. Invest Ophthalmol Vis Sci 1997;38:2711–2720
22. Horio N, Clermont AC, Abiko A, et al. Angiotensin AT(1) receptor antagonism normalizes retinal blood flow and acetylcholine-induced vasodilatation in normotensive diabetic rats. Diabetologia 2004;47:113–123
23. Ravindran S, Grys TE, Welch RA, Schapira M, Patston PA. Inhibition of plasma kallikrein by C1-inhibitor: role of endothelial cells and the amino-terminal domain of C1-inhibitor. Thromb Haemost 2004;92:1277–1283
24. Aiello LP, Bursell SE, Clermont A, et al. Vascular endothelial growth factor-induced retinal permeability is mediated by protein kinase C in vivo and suppressed by an orally effective β-isoform-selective inhibitor. Diabetes 1997;46:1473–1480
25. Lawson SR, Gabra BH, Guérin B, et al. Enhanced dermal and retinal vascular permeability in streptozotocin-induced type 1 diabetes in Wistar rats: blockade with a selective bradykinin B1 receptor antagonist. Regul Pept 2005;124:221–224
26. Abdouh M, Khanjari A, Abdelazziz N, Ongali B, Couture R, Hasséssian HM. Early upregulation of kinin B1 receptors in retinal microvessels of the streptozotocin-diabetic rat. Br J Pharmacol 2003;140:33–40
27. Kedzierska K, Ciechanowski K, Gołembiewska E, et al. Plasma prekallikrein as a risk factor for diabetic retinopathy. Arch Med Res 2005;36:539–543
28. Tschöpe C, Reinecke A, Seidl U, et al. Functional, biochemical, and molecular investigations of renal kallikrein-kinin system in diabetic rats. Am J Physiol 1999;277:H2333–H2340
29. Sharma JN, Kesavarao U. Changes in plasma prekallikrein activity, blood pressure, and left ventricular thickness in hypertensive and normotensive diabetic rats. Methods Find Exp Clin Pharmacol 2007;29:75–78
30. Lawson SR, Gabra BH, Nantel F, Battistini B, Sirois P. Effects of a selective bradykinin B1 receptor antagonist on increased plasma extravasation in streptozotocin-induced diabetic rats: distinct vasculopathic profile of major key organs. Eur J Pharmacol 2005;514:69–78
31. Bursell SE, Clermont AC, Aiello LP, et al. High-dose vitamin E supplementation normalizes retinal blood flow and creatinine clearance in patients with type 1 diabetes. Diabetes Care 1999;22:1245–1251
32. Nagaoka T, Sato E, Takahashi A, Yokota H, Sogawa K, Yoshida A. Impaired retinal circulation in patients with type 2 diabetes mellitus: retinal laser doppler velocimetry study. Invest Ophthalmol Vis Sci 2010;51:6729–6734
33. Burgansky-Eliash Z, Nelson DA, Bar-Tal OP, Lowenstein A, Grinvald A, Barak A. Reduced retinal blood flow velocity in diabetic retinopathy. Retina 2010;30:765–773
34. Harpel PC. Studies on the interaction between collagen and a plasma kallikrein-like activity. Evidence for a surface-active enzyme system. J Clin Invest 1972;51:1813–1822
35. Schousboe I, Nystrøm B. High molecular weight kininogen binds to laminin: characterization and kinetic analysis. FEBS J 2009;276:5228–5238
36. Maas C, Govers-Riemslag JW, Bouma B, et al. Misfolded proteins activate factor XII in humans, leading to kallikrein formation without initiating coagulation. J Clin Invest 2008;118:3208–3218
37. Joseph K, Tholanikunnel BG, Kaplan AP. Heat shock protein 90 catalyzes activation of the prekallikrein-kininogen complex in the absence of factor XII. Proc Natl Acad Sci U S A 2002;99:896–900
38. Liu J, Gao BB, Feener EP. Proteomic identification of novel plasma kallikrein substrates in the astrocyte secretome. Transl Stroke Res 2010;1:276–286
39. Yeung L, Lima VC, Garcia P, Landa G, Rosen RB. Correlation between spectral domain optical coherence tomography findings and fluorescein angiography patterns in diabetic macular edema. Ophthalmology 2009;116:1158–1167